

# Semi-Automatic Task Graph Construction for $\mathcal{H}$ -Matrix Arithmetic

Steffen Börm  
Department of Mathematics  
University of Kiel  
boerm@math.uni-kiel.de

Sven Christophersen  
Department of Mathematics  
University of Kiel  
christophersen@math.uni-kiel.de

Ronald Kriemann  
MPI for Mathematics i.t.S.  
Leipzig, Germany  
rok@mis.mpg.de

July 6, 2021

**Abstract** A new method to construct task graphs for  $\mathcal{H}$ -matrix arithmetic is introduced, which uses the information associated with all tasks of the standard recursive  $\mathcal{H}$ -matrix algorithms, e.g., the block index set of the matrix blocks involved in the computation. Task refinement, i.e., the replacement of tasks by sub-computations, is then used to proceed in the  $\mathcal{H}$ -matrix hierarchy until the matrix blocks containing the actual matrix data are reached. This process is a natural extension of the classical, recursive way in which  $\mathcal{H}$ -matrix arithmetic is defined and thereby simplifies the efficient usage of many-core systems. Examples for standard and accumulator based  $\mathcal{H}$ -arithmetic are shown for model problems with different block structures.

**AMS Subject Classification:** 65F05, 65Y05, 65Y20, 68W10, 68W40

**Keywords:** hierarchical matrices, task graph, parallel algorithms, many-core processors

## 1 Introduction

Hierarchical matrices ( $\mathcal{H}$ -matrices), introduced in [15], are a powerful tool to represent dense matrices coming from integral equations or partial differential equations in a hierarchical, block-oriented, data-sparse way with log-linear memory costs. Furthermore, a matrix arithmetic, e.g., matrix addition, multiplication, inversion and factorization, is possible with log-linear computation costs (see [13]).

Classical arithmetic for  $\mathcal{H}$ -matrices is formulated recursively following the recursive block structure of the matrices. This formulation has the advantage of simplicity, since only local blocks are addressed, e.g., the sub blocks of the current matrix block, and therefore the implementation only needs to handle a few of them. The latter also simplifies the analysis of the arithmetic and their implementation.

In [3] a modified formulation of the  $\mathcal{H}$ -arithmetic was introduced, which collects all updates to sub blocks in *accumulators*, thereby postponing the modification of those sub blocks only after all updates are available. Furthermore, the application of these accumulated updates strictly fol-

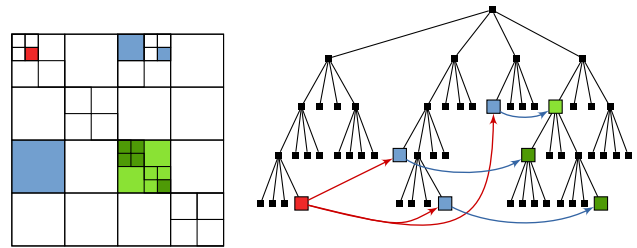


Figure 1:  $\mathcal{H}$ -matrix (left) and dependencies of matrix blocks during  $\mathcal{H}$ -LU in tree structure (right).

lows the hierarchy of the  $\mathcal{H}$ -matrix, pushing updates to structured matrix blocks only to the next level below. With this, the number of updates applied to leaf blocks of the  $\mathcal{H}$ -matrix is reduced and such also the number of low-rank truncations. This significantly improves the runtimes of  $\mathcal{H}$ -arithmetic.

Due to the substantial changes in the hardware landscape in the last decade, e.g., with many-core CPUs integrating 64 and more cores into a single CPU, e.g., AMD Epyc 7002 series, the implementation of  $\mathcal{H}$ -matrix arithmetic also needs to efficiently make use of thread-level parallelism to speed up the  $\mathcal{H}$ -matrix computations. However, using the recursive functions and applying parallelization on the local level as used in [19] introduces too much artificial synchronisation points to be efficient with such a high number of CPU cores.

Therefore, a different strategy is used for many-core CPUs based on *tasks* to describe the atomic computation blocks and their dependencies which form a directed acyclic graph (DAG). This task graph is handed to a scheduling system to execute a task when all its dependencies are met on the next free CPU core. Such task-based approaches were also used for dense [8, 9] and sparse [17, 22, 7] arithmetic and previously described in [20] for  $\mathcal{H}$ -matrices.

The remaining problem is to construct the DAG for the runtime scheduling system. Constructing the DAG includes identification of the compute tasks and especially their de-

dependencies. Normally, both are based on the arithmetical formulation of the data the tasks work on. For many dense or sparse matrix algorithms without a complex recursive hierarchy, the dependencies can often be directly expressed, e.g., based on matrix blocks or coefficient indices. For  $\mathcal{H}$ -matrix arithmetic, it is more complicated because the matrix blocks are defined on different levels of the hierarchy. An example is shown in Figure 1. There, for the  $\mathcal{H}$ -LU factorization, the red diagonal block forms a dependency for the blue blocks, which for themselves form a dependency for the updates of the green matrix blocks. In the corresponding tree representing the relation between all matrix blocks, the blocks are on different levels and not necessarily close to each other. The connecting paths may go back to the root of the tree. Furthermore, inner blocks of the tree do not correspond to actual data, as this is stored only at the leaf blocks, and hence the computation affects all sub-blocks, thereby creating more dependencies.

This is the reason why in [20], the traditional formulation of  $\mathcal{H}$ -matrix arithmetic was changed to have a *level-wise*, global view of the matrix similar to single level dense arithmetic, i.e., on each level of the hierarchy, all matrix blocks in a block row or column were used to set up dependencies. The resulting task graph represented data dependency over the whole  $\mathcal{H}$ -matrix and permitted to schedule ready tasks independent of the position in the matrix without unnecessary task synchronisation. However, the modified  $\mathcal{H}$ -matrix arithmetic formulation requires extra data to permit access to all needed matrix blocks and the process of defining the task graph was error-prone, which hinders the implementation of DAGs for new arithmetic functions.

A more natural way of defining the DAG would be to follow the standard, recursive  $\mathcal{H}$ -matrix functions. However, this would require to handle nested task parallelism with dependencies over different recursion paths. Various task runtime scheduling systems exist which try to address this problem. The most widely used of such systems is OpenMP [11], which introduced tasks in v3 and extended this by task dependencies in v4 [23], where data input/output dependencies are defined by memory ranges (memory address plus length). Though this works well for single-level algorithms, dependencies between sub-tasks in different recursion paths are difficult to implement<sup>1</sup>

The same limitations apply to the OmpSs [5] parallelization framework, which introduced the task system before OpenMP. Despite these restrictions, OmpSs was used in [1] to construct task graphs for  $\mathcal{H}$ -matrix arithmetic. However, only a very restricted, non-efficient version of  $\mathcal{H}$ -matrix arithmetic was possible.

In [24] an extension to OpenMP, implemented in OmpSs-2 [6], was introduced, which distinguishes between standard and *weak* dependencies. A weak dependency from a

parent task to a sub-task does not require the parent task to wait for the sub-task to finish as would be needed in OmpSs (or OpenMP) thereby avoiding unnecessary task synchronisation. This extension would permit the implementation of nested functions with fine grained dependencies as the  $\mathcal{H}$ -matrix arithmetic makes use of and was used in [10] to fully implement task-based  $\mathcal{H}$ -matrix arithmetic. The presented numerical results demonstrate that the technique has some potential but needs further optimizations to be efficient for a wide range of  $\mathcal{H}$ -matrix structures. Furthermore, a special compiler is needed supporting these non-standard features, though it is expected that weak dependencies will eventually be introduced also in OpenMP.

With so called *bubbles of tasks*, StarPU ([2, 25]) tries to address the issue, where tasks are not restricted to wait for sub-tasks to finish but where these sub-tasks may extend data dependencies over the local boundaries as defined by recursion. It is currently unclear, whether this concept is capable of efficiently handling recursive  $\mathcal{H}$ -matrix arithmetic.

Because of these difficulties, we avoid such a general approach and propose a simpler method for  $\mathcal{H}$ -matrix functions, which makes use of data that is coupled with all sub-blocks of  $\mathcal{H}$ -matrices: the block index sets. With the block index sets for all input and output matrices of a function the problem of addressing the actual data storage vanishes as any dependency automatically includes any (leaf) sub-block. Furthermore, corresponding data dependencies are automatically constructed and refined when replacing tasks by sub-tasks, e.g., during function recursion. During the refinement, the dependencies can be filtered based on sub-set tests for the block index sets of the sub-blocks associated with the sub-tasks. This eliminates unneeded dependencies to parent or sibling tasks. As a result, a task graph for  $\mathcal{H}$ -matrix arithmetic is computed which can spawn tasks for leaf blocks as soon as possible and avoids unnecessary synchronization.

Furthermore, since the task graph is constructed without a particular task scheduling system, the new method can be combined with an arbitrary task runtime system. Therefore, for a particular computer system, the best runtime system may be chosen.

This article is structured as follows: in Section 2  $\mathcal{H}$ -matrices and their arithmetic are introduced. The new DAG construction is described in Section 3 with some optimizations presented in Section 4. Section 5 contains the results of several numerical experiments comparing the different approaches.

All presented algorithms are available in the software HLR (see [21]) released under an open-source license.

<sup>1</sup>Fixed hierarchies would permit predefined, static task graphs. Unrestricted hierarchies requiring dynamic task graphs are basically impossible to implement.

## 2 $\mathcal{H}$ -Matrices and $\mathcal{H}$ -Arithmetic

### 2.1 Definitions

For an indexset  $I$  we define the *cluster tree* (or  $\mathcal{H}$ -tree) as the hierarchical partitioning of  $I$  into disjoint sub-sets of  $I$ :

**Definition 2.1 (Cluster Tree)** Let  $T_I = (V, E)$  be a tree with  $V \subset \mathcal{P}(I)$ .  $T_I$  is called a cluster tree over  $I$  if

1.  $I = \text{root}(T_I)$  and
2. for all  $v \in V$  with  $\text{sons}(v) \neq \emptyset$  :  $v = \dot{\cup}_{v' \in \text{sons}(v)} v'$ .

A node in  $T_I$  is also called a cluster and we write  $\tau \in T_I$  if  $\tau \in V$ . The set of leaves of  $T_I$  is denoted by  $\mathcal{L}(T_I)$ .

Similar to a cluster tree we can extend the hierarchical partitioning to the product  $I \times J$  of two index sets  $I, J$ , while restricting the possible set of nodes by given cluster trees  $T_I$  and  $T_J$  over  $I$  and  $J$ , respectively. Furthermore, the set of leaves will be defined by an application dependent *admissibility condition* (see [16] for examples).

**Definition 2.2 (Block Tree)** Let  $T_I, T_J$  be two cluster trees and let  $\text{adm} : T_I \times T_J \rightarrow \mathbb{B}$ . The block tree  $T = T_I \times T_J$  is recursively defined starting with  $\text{root}(T) = (I, J)$ :

$$\text{sons}(\tau, \sigma) = \begin{cases} \emptyset & \text{if } \text{adm}(\tau, \sigma) = \text{true}, \text{sons}(\tau) = \emptyset \text{ or } \text{sons}(\sigma) = \emptyset, \\ \{(\tau', \sigma') : \tau' \in \text{sons}(\tau), \sigma' \in \text{sons}(\sigma)\} & \text{else.} \end{cases}$$

A node in  $T$  is also called a block. Again, the set of leaves of  $T$  is denoted by  $\mathcal{L}(T) := \{b \in T : \text{sons}(b) = \emptyset\}$ .

The admissibility condition ensures that admissible blocks in  $T$ , i.e., blocks  $b$  with  $\text{adm}(b) = \text{true}$ , can be approximated by a predefined rank  $k$  (or up to a predefined accuracy  $\varepsilon$ ). The set of all such matrices forms the set of  $\mathcal{H}$ -matrices:

**Definition 2.3 ( $\mathcal{H}$ -Matrix)** For a block tree  $T$  over cluster trees  $T_I, T_J$  and  $k \in \mathbb{N}$ , the set of  $\mathcal{H}$ -matrices  $\mathcal{H}(T, k)$  is defined as

$$\mathcal{H}(T, k) := \{M \in \mathbb{R}^{I \times J} : \forall (\tau, \sigma) \in \mathcal{L}(T) : \text{rank}(M_{\tau, \sigma}) \leq k \vee \tau \in \mathcal{L}(T_I) \vee \sigma \in \mathcal{L}(T_J)\}$$

Here,  $M_{\tau, \sigma}$  refers to the sub-block  $M|_{\tau \times \sigma}$ .

### 2.2 $\mathcal{H}$ -Arithmetic

For many arithmetical functions the matrix multiplication forms the basic building block. In this work, we will consider the general version

$$C := \alpha A \cdot B + C$$

which applies the update  $\alpha AB$  to the matrix  $C$ . If not stated otherwise, we will assume a binary cluster tree, e.g., for a non-leaf cluster  $t$  we have  $\text{sons}(\tau) = \{\tau_0, \tau_1\}$ , and hence a quad block cluster tree, which will simplify the presentation. The algorithms can easily be extended for general cluster trees.

For an  $\mathcal{H}$ -matrix  $M_{\tau, \sigma} \in \mathcal{H}(T)$  with  $T$  based on a binary tree, the block structure can be written as

$$M = \begin{pmatrix} M_{\tau_0, \sigma_0} & M_{\tau_0, \sigma_1} \\ M_{\tau_1, \sigma_0} & M_{\tau_1, \sigma_1} \end{pmatrix}$$

Using this notation for the above matrix multiplication, the algorithm for the  $\mathcal{H}$ -matrix multiplication can be written recursively as

#### Algorithm 1: $\mathcal{H}$ -Matrix Multiplication

```

procedure hmul(in:  $\alpha, A_{\tau, \rho}, B_{\rho, \sigma}$ , inout:  $C_{\tau, \sigma}$ )
  if  $\{(\tau, \rho), (\rho, \sigma), (\tau, \sigma)\} \cap \mathcal{L}(T) = \emptyset$  then
    for  $i, j, \ell \in \{0, 1\}$  do
      hmul( $\alpha, A_{\tau_i, \rho_\ell}, B_{\rho_\ell, \sigma_j}, C_{\tau_i, \sigma_j}$ );
  else
     $C_{\tau, \sigma} := C_{\tau, \sigma} + \alpha A_{\tau, \rho} B_{\rho, \sigma}$ ;

```

In the non-recursive part, special routines will handle the different multiplications between structured, dense and low-rank matrices.

An only slightly more advanced matrix algorithm is the LU factorization  $A_{\tau, \tau} = L_{\tau, \tau} U_{\tau, \tau}$  of the matrix  $A_{\tau, \tau}$  into triangular factors  $L_{\tau, \tau}$  and  $U_{\tau, \tau}$ . Using the above block structure for the  $\mathcal{H}$ -matrix  $A_{\tau, \tau}$ , this reads

$$\begin{pmatrix} A_{\tau_0, \tau_0} & A_{\tau_0, \tau_1} \\ A_{\tau_1, \tau_0} & A_{\tau_1, \tau_1} \end{pmatrix} = \begin{pmatrix} L_{\tau_0, \tau_0} & \\ & L_{\tau_1, \tau_0} \end{pmatrix} \begin{pmatrix} U_{\tau_0, \tau_0} & U_{\tau_0, \tau_1} \\ & U_{\tau_1, \tau_1} \end{pmatrix}$$

which leads to Algorithm 2 with recursive call in case of structured matrices, using functions `htrsl` and `htrsu` for the matrix solve operations, and a dense LU factorization if the input matrix is dense.

#### Algorithm 2: $\mathcal{H}$ -LU factorization

```

procedure hlu(in:  $A_{\tau, \tau}$ , out:  $L_{\tau, \tau}, U_{\tau, \tau}$ )
  if  $(\tau, \tau) \notin \mathcal{L}(T)$  then
    hlu( $A_{\tau_0, \tau_0}, L_{\tau_0, \tau_0}, U_{\tau_0, \tau_0}$ );
    htrsu( $U_{\tau_0, \tau_0}, A_{\tau_1, \tau_0}, L_{\tau_1, \tau_0}$ );
    htrsl( $L_{\tau_0, \tau_0}, A_{\tau_0, \tau_1}, U_{\tau_0, \tau_1}$ );
    hmul( $-1, L_{\tau_1, \tau_0}, U_{\tau_0, \tau_1}, A_{\tau_1, \tau_1}$ );
    hlu( $A_{\tau_1, \tau_1}, L_{\tau_1, \tau_1}, U_{\tau_1, \tau_1}$ );
  else
    solve  $A_{\tau, \tau} = L_{\tau, \tau} U_{\tau, \tau}$ ;

```

Coming back to the matrix solves,  $L_{\tau, \tau} X_{\tau, \sigma} = M_{\tau, \sigma}$  with a lower triangular matrix  $L_{\tau, \tau}$  can be written using the block structure as

$$\begin{pmatrix} L_{\tau_0, \tau_0} & \\ & L_{\tau_0, \tau_1} \end{pmatrix} \begin{pmatrix} X_{\tau_0, \sigma_0} & X_{\tau_0, \sigma_1} \\ X_{\tau_0, \sigma_1} & X_{\tau_1, \sigma_1} \end{pmatrix} = \begin{pmatrix} M_{\tau_0, \sigma_0} & M_{\tau_0, \sigma_1} \\ M_{\tau_0, \sigma_1} & M_{\tau_1, \sigma_1} \end{pmatrix}$$

With  $M$  being given and  $X$  sought, we obtain the equations for the sub-blocks which can be used to formulate the algorithm for `htrsl` as shown in Algorithm 3.

**Algorithm 3:** Lower triangular  $\mathcal{H}$ -matrix solve

```

procedure htrsl(in:  $L_{\tau,\tau}, M_{\tau,\sigma}$ , out:  $X_{\tau,\sigma}$ )
  if  $(\tau, \sigma) \notin \mathcal{L}(T)$  then
    htrsl( $L_{\tau_0,\tau_0}, M_{\tau_0,\sigma_0}, X_{\tau_0,\sigma_0}$ );
    htrsl( $L_{\tau_0,\tau_0}, M_{\tau_0,\sigma_1}, X_{\tau_0,\sigma_1}$ );
    hmul( $-1, L_{\tau_1,\tau_0}, X_{\tau_0,\sigma_0}, M_{\tau_1,\sigma_0}$ );
    hmul( $-1, L_{\tau_1,\tau_0}, X_{\tau_0,\sigma_1}, M_{\tau_1,\sigma_1}$ );
    htrsl( $L_{\tau_1,\tau_1}, M_{\tau_1,\sigma_0}, X_{\tau_1,\sigma_0}$ );
    htrsl( $L_{\tau_1,\tau_1}, M_{\tau_1,\sigma_1}, X_{\tau_1,\sigma_1}$ );
  else
    solve  $L_{\tau,\tau} X_{\tau,\sigma} = M_{\tau,\sigma}$ ;

```

Similarly, the function `htrs` for solving  $X_{\sigma,\tau} U_{\tau,\tau} = M_{\sigma,\tau}$  with an upper triangular matrix block  $U_{\tau,\tau}$  can be implemented.

### 2.3 Accumulator based Arithmetic

In the formulation of `hmul` each update in the non-recursive part is applied to the destination matrix  $C_{\tau,\sigma}$  as soon as possible in standard implementations of  $\mathcal{H}$ -matrix arithmetic. For low-rank matrices  $C_{\tau,\sigma}$ , each of these updates involve a truncation operation to reduce the rank of the sum  $C_{\tau,\sigma} + \alpha A_{\tau,\rho} B_{\rho,\sigma}$  to the predefined rank  $k$  or precision  $\varepsilon$ .

Such updates to low-rank matrices may also occur if  $C$  is a structured matrix and  $\alpha A_{\tau,\rho} B_{\rho,\sigma}$  is a low-rank update, e.g., if either  $A_{\tau,\rho}$  or  $B_{\rho,\sigma}$  corresponds to a low-rank matrix. In this case, all leaf sub-blocks of  $C_{\tau,\sigma}$  will be updated. Again, each of those updates is applied individually in typical implementation for  $\mathcal{H}$ -matrix arithmetic. This often leads to a significant number of truncation operations for low-rank blocks within an  $\mathcal{H}$ -matrix.

In [3], a different approach was described, where updates are collected level-wise in a separate matrix, called *accumulator*. After all updates per level are applied, these collected updates are shifted down to the accumulators of the matrix blocks of the next level. The process is then repeated until the leaf blocks in the matrix are reached. At this point all updates to the destination block have been collected in the corresponding accumulator matrix and are applied in a single update step.

By collecting updates per level, the number of truncation operations can be reduced significantly. Since these contribute to a large part of the overall runtime of typical  $\mathcal{H}$ -arithmetic functions, this also leads to faster algorithms.

**Remark 2.4** A related modification of the  $\mathcal{H}$ -arithmetic was introduced in [12] where updates are also postponed until the leaf matrix blocks need to be modified. In contrast to the accumulator based  $\mathcal{H}$ -arithmetic, the updates in [12] are not accumulated per level of the block tree but all updates are shifted to the leaves.

For  $C_{\tau,\sigma}$  the accumulator matrix shall be denoted by  $\mathcal{U}_{\tau,\sigma}$ .  $\mathcal{U}_{\tau,\sigma}$  will contain the sum of all updates to  $C_{\tau,\sigma}$  for which  $\alpha A_{\tau,\rho} B_{\rho,\sigma}$  results in a low-rank or dense matrix and the update can be applied directly. If  $\alpha A_{\tau,\rho} B_{\rho,\sigma}$  results in a structured matrix, the application will be deferred to sub-blocks of  $C_{\tau,\sigma}$ , which corresponds to the recursive step of Algorithm 1. Such updates will be stored in the set  $\mathcal{P}_{\tau,\sigma}$  of *pending* updates.

The storage format of  $\mathcal{U}_{\tau,\sigma}$  is left open. By default, a low-rank representation in factorised form is used, where  $\mathcal{U}_{\tau,\sigma}$  will not need storage space at the start of the arithmetic because  $\text{rank}(\mathcal{U}_{\tau,\sigma}) = 0$ . However, for optimisation reasons, a dense storage format may be more efficient if dense updates to  $C_{\tau,\sigma}$  occur.

For the accumulator arithmetic, the handling of updates of the form  $C_{\tau,\sigma} := C_{\tau,\sigma} + \alpha A_{\tau,\rho} B_{\rho,\sigma}$  is split into two steps, represented by different functions. The first step is implemented by `add_upd`, which collects the update  $\alpha A_{\tau,\rho} B_{\rho,\sigma}$  and either applies it to the accumulator  $\mathcal{U}_{\tau,\sigma}$  if the product can be evaluated or stores the tuple  $(\alpha, A_{\tau,\rho}, B_{\rho,\sigma})$  in the set  $\mathcal{P}_{\tau,\sigma}$  of pending updates.

**Algorithm 4:** Collect single update

```

procedure add_upd(in:  $\alpha, A_{\tau,\rho}, B_{\rho,\sigma}, C_{\tau,\sigma}$ )
  if  $\{(\tau, \rho), (\rho, \sigma), (\tau, \sigma)\} \cap \mathcal{L}(T) = \emptyset$  then
     $\mathcal{P}_{\tau,\sigma} := \mathcal{P}_{\tau,\sigma} \cup \{(\alpha, A_{\tau,\rho}, B_{\rho,\sigma})\}$ ;
  else
     $\mathcal{U}_{\tau,\sigma} := \mathcal{U}_{\tau,\sigma} + \alpha \cdot A_{\tau,\rho} \cdot B_{\rho,\sigma}$ ;

```

The second step consists of shifting down the collected updates in  $\mathcal{U}_{\tau,\sigma}$  and  $\mathcal{P}_{\tau,\sigma}$  to sub-blocks in case of structured matrices or applying the accumulated updates to the leaf matrix  $C_{\tau,\sigma}$ , and is shown in Algorithm 5 in function `apply_upd`. The actual update shift is implemented in Algorithm 6. There, for pending updates the individual update factors are split, corresponding to the triple-loop in Algorithm 1.

**Algorithm 5:** Apply all collected updates

```

procedure apply_upd(in:  $C_{\tau,\sigma}$ )
  if  $(\tau, \sigma) \notin \mathcal{L}(T)$  then
    shift_upd( $C_{\tau,\sigma}$ );
    for  $\tau' \in \text{sons}(\tau), \sigma' \in \text{sons}(\sigma)$  do
      apply_upd( $C_{\tau',\sigma'}$ );
  else
     $C_{\tau,\sigma} := C_{\tau,\sigma} + \mathcal{U}_{\tau,\sigma}$ ;

```

**Algorithm 6:** Shift accumulated updates to sub-blocks

```

procedure shift_upd(in:  $C_{\tau,\sigma}$ )
  for  $\tau' \in \text{sons}(\tau), \sigma' \in \text{sons}(\sigma)$  do
     $\mathcal{U}_{\tau',\sigma'} := \mathcal{U}_{\tau',\sigma'} + \mathcal{U}_{\tau,\sigma|_{\tau',\sigma'}}$ ;
    for  $(\alpha, A_{\tau,\rho}, B_{\rho,\sigma}) \in \mathcal{P}_{\tau,\sigma}, \rho' \in \text{sons}(\rho)$  do
      add_upd( $\alpha, A_{\tau',\rho'}, B_{\rho',\sigma'}, C_{\tau',\sigma'}$ );

```

With these functions, the standard  $\mathcal{H}$ -matrix multiplication  $C := C + AB$  is evaluated by replacing the function call

```
hmul(1, A, B, C);
```

by

```
add_upd(1, A, B, C);
apply_upd(C);
```

For the  $\mathcal{H}$ -LU factorization, one could follow the same scheme and replace the function `hmul` by the corresponding functions `add_upd` and `apply_upd`. However, this might fail to collect all updates before applying the accumulator to the destination matrix block. The reason is, that on a single level in the  $\mathcal{H}$ -LU factorization, multiple `hmul` calls may occur to the same destination, e.g., if the block structure is not only  $2 \times 2$ . Also, updates from different recursion levels of the LU factorization are not handled.

Instead, collection and application of updates are split during  $\mathcal{H}$ -LU. Each call to `hmul` will be replaced by `add_upd`, e.g., only collecting the updates. If a recursive step occurs during  $\mathcal{H}$ -LU, the accumulated updates are shifted down to all sub-blocks with `shift_upd`, thereby ensuring that all sub-blocks will have all collected updates from the upper levels. For leaf matrix blocks, the updates are applied before (dense) factorization using `apply_upd`.

#### Algorithm 7: $\mathcal{H}$ -LU factorization with accumulators

```

procedure hlu(in:  $A_{\tau,\tau}$ , out:  $L_{\tau,\tau}, U_{\tau,\tau}$ )
  if  $(\tau, \tau) \notin \mathcal{L}(T)$  then
    shift_upd( $A_{\tau,\tau}$ );
    hlu( $A_{\tau_0,\tau_0}, L_{\tau_0,\tau_0}, U_{\tau_0,\tau_0}$ );
    htrsu( $U_{\tau_0,\tau_0}, A_{\tau_1,\tau_0}, L_{\tau_1,\tau_0}$ );
    htrsl( $L_{\tau_0,\tau_0}, A_{\tau_0,\tau_1}, U_{\tau_0,\tau_1}$ );
    add_upd(-1,  $L_{\tau_1,\tau_1}, U_{\tau_1,\tau_1}, A_{\tau_1,\tau_1}$ );
    hlu( $A_{\tau_1,\tau_1}, L_{\tau_1,\tau_1}, U_{\tau_1,\tau_1}$ );
  else
    apply_upd( $A_{\tau,\tau}$ );
     $A_{\tau,\tau} = L_{\tau,\tau} U_{\tau,\tau}$ ;

```

The same strategy is applied for the matrix solve functions, e.g., only collect updates whenever `hmul` is called and shift (apply) updates at each recursive (non-recursive) step.

## 3 Task based $\mathcal{H}$ -Arithmetic

### 3.1 Task refinement

For all  $\mathcal{H}$ -matrix arithmetic functions  $f$ , e.g., `hmul` or `hlu`, we can define a corresponding task  $\mathbf{task}(f)$ . For simplicity, we will subsequently identify the  $\mathcal{H}$ -arithmetic function with its task, e.g., write `hlu` instead of  $\mathbf{task}(\mathbf{hlu})$ , if no ambiguity between both concepts exists.

Due to the recursive nature of the  $\mathcal{H}$ -arithmetic functions, they will produce *sub-tasks*, i.e., all subsequent function calls within such an arithmetic function, which will *replace*

#### Algorithm 8: Lower Triangular $\mathcal{H}$ -Matrix Solve with Accumulators

```

procedure htrsl(in:  $L_{\tau,\tau}, M_{\tau,\sigma}$ , out:  $X_{\tau,\sigma}$ )
  if  $(\tau, \sigma) \notin \mathcal{L}(T)$  then
    shift_upd( $M_{\tau,\sigma}$ );
    htrsl( $L_{\tau_0,\tau_0}, M_{\tau_0,\sigma_0}, X_{\tau_0,\sigma_0}$ );
    htrsl( $L_{\tau_0,\tau_0}, M_{\tau_0,\sigma_1}, X_{\tau_0,\sigma_1}$ );
    add_upd(-1,  $L_{\tau_1,\tau_0}, X_{\tau_0,\sigma_0}, M_{\tau_1,\sigma_0}$ );
    add_upd(-1,  $L_{\tau_1,\sigma_0}, X_{\tau_0,\sigma_1}, M_{\tau_1,\sigma_1}$ );
    htrsl( $L_{\tau_1,\tau_1}, M_{\tau_1,\sigma_0}, X_{\tau_1,\sigma_0}$ );
    htrsl( $L_{\tau_1,\tau_1}, M_{\tau_1,\sigma_1}, X_{\tau_1,\sigma_1}$ );
  else
    apply_upd( $M_{\tau,\sigma}$ );
    solve  $L_{\tau,\tau} X_{\tau,\sigma} = M_{\tau,\tau}$ ;

```

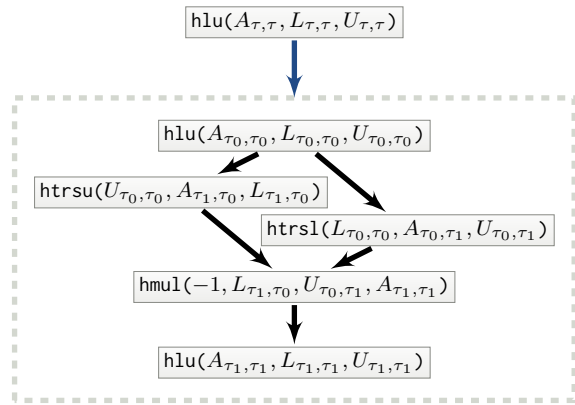


Figure 2: Task refinement and resulting sub-tasks of  $\mathbf{hlu}(A_{\tau,\tau}, L_{\tau,\tau}, U_{\tau,\tau})$ .

the original task. In Figure 2 this is shown for the function `hlu`.

For a task  $t$ , let  $V_t$  be the set of sub-tasks. The tasks  $t' \in V_t$  will have a data dependency relation between them, e.g., output data of one task is needed as the input of another task.

We can formalise these data dependencies in the context of  $\mathcal{H}$ -matrices with the help of the matrix blocks the corresponding tasks work on. Each of these matrix blocks is identified by block index sets  $\tau \times \sigma \in T$ . For the function `hlu` those blocks are  $A_{\tau,\tau}$ ,  $L_{\tau,\tau}$  and  $U_{\tau,\tau}$ , with input data defined by  $A_{\tau,\tau}$  and output data defined by  $L_{\tau,\tau}$  and  $U_{\tau,\tau}$ . For the  $\mathcal{H}$ -arithmetic tasks we will identify these matrix blocks as a pair consisting of the corresponding block index set and an identifier representing the (global) matrix, e.g.,  $A$ ,  $L$  or  $U$ .

**Definition 3.1 (Data Dependencies)** *Let  $\mathcal{I}$  be a set of identifiers and let  $\text{id}$  denote the mapping of matrices to their identifiers. For each task  $t$  let  $t_{\text{in}} \subset \mathcal{I} \times V(T)$  denote the set of input data dependencies and  $t_{\text{out}} \subset \mathcal{I} \times V(T)$  the set of output data dependencies, respectively.*

In Table 1 the sets of input/output data dependencies is



shown for the previously introduced  $\mathcal{H}$ -matrix functions.

Based on the data dependencies the task dependencies can be defined:

**Definition 3.2 (Task Dependencies)** Let  $t^i \neq t^j$  be two tasks. We say that  $t^i$  precedes  $t^j$ , written as  $t^i \rightarrow t^j$ , iff

$$\exists(\text{id}^i, b^i) \in t_{\text{out}}^i, (\text{id}^j, b^j) \in t_{\text{in}}^j : \text{id}^i = \text{id}^j \wedge b^i \cap b^j \neq \emptyset.$$

Furthermore, for any task  $t$  let  $S_t \subseteq \mathcal{T}$  be the set of successors of  $t$ , e.g.,  $S_t := \{g : t \rightarrow g\}$ .

For the general case, we assume that the sub tasks  $V_t$  and the dependencies  $E_t \subset V_t \times V_t$  between tasks in  $V_t$ , forming a local graph  $G_t = (V_t, E_t)$ , are user-provided for each task  $t$ . Normally, these directly follow from the definition of the standard  $\mathcal{H}$ -arithmetic functions, e.g., instead of a function call, a sub-task is created (cf. Figure 2).

**Remark 3.3** It is important that  $G_t$  must not include a loop in the corresponding task graph. Otherwise, the result of the task graph generation below will not produce a DAG, as is needed for the execution phase of the task graph.

**Remark 3.4** For many  $\mathcal{H}$ -matrix algorithms, including  $\mathcal{H}$ -LU, the construction of  $E_t$  can be automated by comparing the input/output data dependencies of the sub-tasks in  $V_t$ , which further simplifies the whole process of task graph generation.

After all tasks are refined and the sub-tasks together with their local dependencies are given, the next step is to set up the task dependencies between sub-tasks of tasks  $t, g$  with  $t \rightarrow g$ . This can be done automatically using the data dependencies of the sub-tasks. Let  $V_t = \{t_1, t_2\}$ . Then also  $t_1 \rightarrow g$  and  $t_2 \rightarrow g$  holds. However, if  $g$  is refined, i.e.,  $V_g = \{g_1, g_2\}$ , the task dependencies  $t_1 \rightarrow g_1, t_1 \rightarrow g_2, t_2 \rightarrow g_1$  and  $t_2 \rightarrow g_2$  do not necessarily apply. Therefore, when refining tasks and by that also their dependencies, only those task dependencies as due to Definition 3.2 will remain. Algorithm 9 performs this comparison of sub-tasks to restrict the dependency set. An example of the result for the  $\mathcal{H}$ -LU factorization is shown in Figure 3.

**Algorithm 9:** Inheritance and refinement of sub-task dependencies

```

procedure refine_sub_deps(in:  $t$ , out:  $E$ )
  for  $g \in S_t$  do
    if  $V_g \neq \emptyset$  then  $S := V_g$ ;
    else  $S := \{g\}$ ;
    for  $t' \in V_t, s \in S$  do
      if  $t' \rightarrow s$  then
         $E := E \cup \{(t', s)\}$ ;

```

The same dependency refinement also has to be performed if the task  $t$  is not refined but  $g$  is, e.g., replacing  $t \rightarrow g$  by  $\{t \rightarrow g_1, t \rightarrow g_2\}$ . The corresponding algorithm

**Algorithm 10:** Refinement of local task dependencies

```

procedure refine_loc_deps(in:  $t$ , out:  $E$ )
  for  $g \in S_t$  do
    if  $V_g \neq \emptyset$  then  $S := V_g$ ;
    else  $S := \{g\}$ ;
    for  $s \in S$  do
      if  $t \rightarrow s$  then
         $E := E \cup \{(t, s)\}$ ;

```

works in an analog way to Algorithm 9 and is shown in Algorithm 10.

For the computation of the task graph, both steps, e.g., task refinement and dependency refinement, are now put together in an iterative process as is shown in Algorithm 11. In each step, first the current tasks are refined (assuming user-provided sub-tasks and sub-task dependencies), followed by the refinement of the inherited dependencies. If after both steps, a task was neither refined nor any of its successor task were, it will not change in further iteration steps and may be removed from the workset of subsequent loops. If no task remains to be refined, the iteration finishes. The number of iterations is given by  $\text{depth}(\mathcal{T})$ . The start of the computation is defined by the single task for the top-level call to the  $\mathcal{H}$ -arithmetic function, e.g.,  $\text{hlu}(A, L, U)$ .

**Remark 3.5** In practise, it may be more efficient to stop the iteration if the tasks are too small, e.g., if the overhead of handling the tasks outweighs the computation performed within the tasks. This may either be done by stopping the recursion before reaching  $\text{depth}(\mathcal{T})$  or by stopping the refinement of tasks at a user-specified matrix block size.

**Algorithm 11:** Computation of task graph

```

procedure compute_dag(in:  $t$ , out:  $G = (V, E)$ )
   $N := \{t\}$ ;  $V := \emptyset$ ;  $E := \emptyset$ ;
  while  $N \neq \emptyset$  do
    for all  $g \in N$  do
      generate  $V_g, E_g$ ;
     $N' := \emptyset$ ;
    for all  $g \in N$  do
      if  $V_g = \emptyset$  then
         $\tilde{S}_g := S_g$ ;
        refine_loc_deps( $g$ );
        if  $S_g \neq \tilde{S}_g$  then
           $N' := N' \cup \{g\}$ ;
        else
           $V := V \cup \{g\}$ ;
           $E := E \cup \{g\} \times S_g$ ;
      else
        refine_sub_deps( $g$ );
         $N' := N' \cup V_g$ ;
     $N := N'$ ;

```

The result  $G = (V, E)$  of Algorithm 11 is a DAG for the

Task	$t_{in}$	$t_{out}$
$hlu(A_{\tau,\tau}, L_{\tau,\tau}, U_{\tau,\tau})$	$\{(id(A), \tau \times \tau)\}$	$\{(id(L), \tau \times \tau), (id(U), \tau \times \tau)\}$
$htrsl(L_{\tau,\tau}, M_{\tau,\sigma}, X_{\tau,\sigma})$	$\{(id(L), \tau \times \tau), (id(M), \tau \times \sigma)\}$	$\{(id(X), \tau \times \sigma)\}$
$htrsu(U_{\tau,\tau}, M_{s,t}, X_{s,t})$	$\{(id(U), \tau \times \tau), (id(M), \sigma \times \tau)\}$	$\{(id(X), \sigma \times \tau)\}$
$hmul(A_{t,r}, B_{r,s}, C_{\tau,\sigma})$	$\{(id(A), \tau \times \rho), (id(B), \rho \times \sigma)\}$	$\{(id(C), \tau \times \sigma)\}$

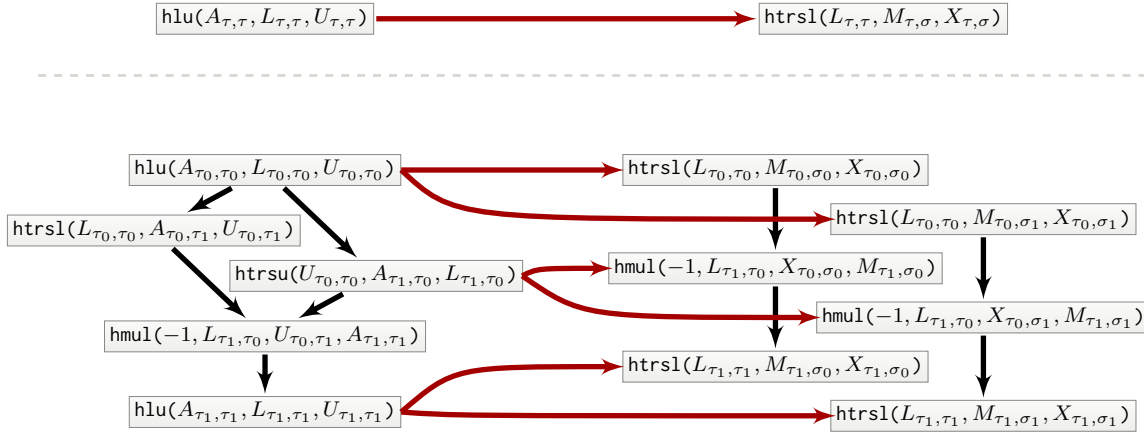
Table 1: Input/output Dependencies for  $\mathcal{H}$ -LU tasks.

Figure 3: Dependencies between parent tasks (top) and refined tasks (bottom).

$\mathcal{H}$ -arithmetic function. An example for the  $\mathcal{H}$ -LU factorization is shown in Figure 4. There, the red nodes correspond to the factorization of diagonal matrix blocks. Off-diagonal matrix solves are colored blue while matrix updates are shown in green.

### 3.2 Task graph with accumulators

If accumulator-based arithmetic is used, the principles of task graph generation remain the same. Only the tasks and their data dependencies will change, e.g., tasks for `add_upd`, `shift_upd` and `apply_upd` have to be generated according to Algorithms 7 and 8.

As for the data dependencies, the arithmetic functions for factorization and matrix solves depend now on the accumulator of the matrix block (due to `shift_upd` and `apply_upd`). In contrast to the matrices  $A$ ,  $L$  and  $U$  these accumulators are distinct matrices, e.g., not being sub-blocks of each other. This leads to identifiers in the data dependencies unique to each accumulator. Since `apply_upd` modifies the actual matrix, the identifier of the output data dependency is again the identifier of the global matrix. The dependency to the accumulator of the parent matrix in `shift_upd` and `apply_upd` ensures the top-down hierarchy of the application of updates via accumulators. Table 2 shows the (modified) data dependencies for the corresponding tasks.

In Figure 5 the task graph for the  $\mathcal{H}$ -LU factorization with accumulators is shown. The tasks for applying updates are marked yellow, while factorization tasks and matrix solve tasks are again red and blue, respectively. The green update

tasks in Figure 4 are replaced by (equally colored) tasks for `add_upd`.

## 4 Optimization Techniques

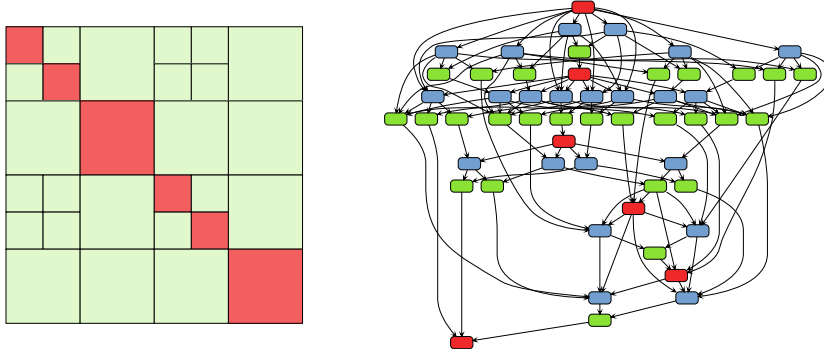
The above introduced task graph generation algorithm provides room for further optimization, where the goals are improved memory requirements (Sections 4.1) and runtime (Section 4.2). Section 4.3 shows an alternative way to incorporate accumulator arithmetic into standard  $\mathcal{H}$ -arithmetic, thereby also reducing the computational cost of task graph generation.

### 4.1 Edge Sparsification

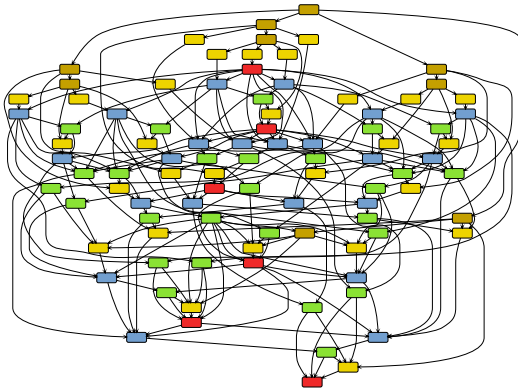
During dependency refinement, the relation  $\rightarrow$  may result in unnecessary edges in  $G$ , e.g. edges  $(t, g) \in E$  for tasks reachable by paths  $t = t_1, t_2, \dots, t_\ell = g, (t_i, t_{i+1}) \in E, 1 \leq i \leq \ell - 1$ . Often this is induced by the hierarchy of the  $\mathcal{H}$ -matrix.

An example of this is shown in Figure 6. There, the off-diagonal matrix solve of block  $A_{\tau_0, \tau_1}$  depends on the factorization of block  $A_{\tau_0, \tau_0}$ . During task refinement all sub-tasks of the factorization of  $A_{\tau_0, \tau_0}$  form a dependency for the matrix solve task. However, since the factorization of  $A_{\tau_0, \tau_0}$  is only finished with the factorization of  $A_{\tau_{01}, \tau_{01}}$ , only the dependency from this task is needed.

Another source of unnecessary edges might be the use of automatic task dependency generation for local sub-tasks

Figure 4:  $\mathcal{H}$ -matrix (left) and corresponding DAG for  $\mathcal{H}$ -LU factorization (right).

Function	$t_{\text{in}}$	$t_{\text{out}}$
$\text{hlu}(A_{\tau,\tau}, L_{\tau,\tau}, U_{\tau,\tau})$	$\{(\text{id}(A), \tau \times \tau),$ $(\text{id}(\text{parent}(A_{\tau,\tau})), \tau \times \tau)\}$	$\{(\text{id}(L), \tau \times \tau), (\text{id}(U), \tau \times \tau)\}$
$\text{htrsl}(L_{\tau,\tau}, M_{\tau,\sigma}, X_{\tau,\sigma})$	$\{(\text{id}(L), \tau \times \tau), (\text{id}(M), \tau \times \sigma),$ $(\text{id}(\text{parent}(M_{\tau,\sigma})), \tau \times \sigma)\}$	$\{(\text{id}(X), \tau \times \sigma)\}$
$\text{htrsU}(U_{\tau,\tau}, M_{\sigma,\tau}, X_{\sigma,\tau})$	$\{(\text{id}(U), \tau \times \tau), (\text{id}(M), \sigma \times \tau),$ $(\text{id}(\text{parent}(M_{\sigma,\tau})), \sigma \times \tau)\}$	$\{(\text{id}(X), \sigma \times \tau)\}$
$\text{add\_upd}(\alpha, A_{\tau,\rho}, B_{\rho,\sigma}, C_{\tau,\sigma})$	$\{(\text{id}(A), \tau \times \rho), (\text{id}(B), \rho \times \sigma)\}$	$\{(\text{id}(C), \tau \times \sigma), (\text{id}(C_{\tau,\sigma}), \tau \times \sigma)\}$
$\text{shift\_upd}(C_{\tau,\sigma})$	$\{(\text{id}(\text{parent}(C_{\tau,\sigma})), \tau \times \sigma),$ $(\text{id}(C_{\tau,\sigma}), \tau \times \sigma)\}$	$\{(\text{id}(C_{\tau,\sigma}), \tau \times \sigma)\}$
$\text{apply\_upd}(C_{\tau,\sigma})$	$\{(\text{id}(\text{parent}(C_{\tau,\sigma})), \tau \times \sigma),$ $(\text{id}(C_{\tau,\sigma}), \tau \times \sigma)\}$	$\{(\text{id}(C), \tau \times \sigma)\}$

Table 2: Input/Output Dependencies for  $\mathcal{H}$ -LU functions using accumulators.Figure 5:  $\mathcal{H}$ -LU-DAG with accumulators.

(see Remark 3.4).

Though these redundant edges have no influence on the correctness of the DAG in terms of execution precedence, they increase the number of edges of the DAG and by this its memory requirements. Furthermore, the runtime of the task graph generation is higher since more edges have to be processed.

During task and dependency refinement, redundant edges are not generated between arbitrary nodes in  $G$  since refinement only affects neighbours of the corresponding tasks or of the sub-tasks. Therefore, a reachability test between a task and nodes in its neighbourhood after a refinement step can detect such unneeded edges, e.g., if a path  $t, \dots, g$  of length at least two exists between  $t$  and  $g$ , the edge  $(t, g) \in E$  can be removed from the graph. This is implemented in Algorithm 12 where for a node  $t$  (or all its sub-nodes) all non-direct descendants, reachable within a given neighbourhood are determined. If for such a descendant  $s$  also an edge  $(t, s)$  exists, this edge will be removed.

The neighbourhood is determined by the task and its successor tasks (or their sub-tasks). In case of a refined task, all sub-tasks and their successors define the possible



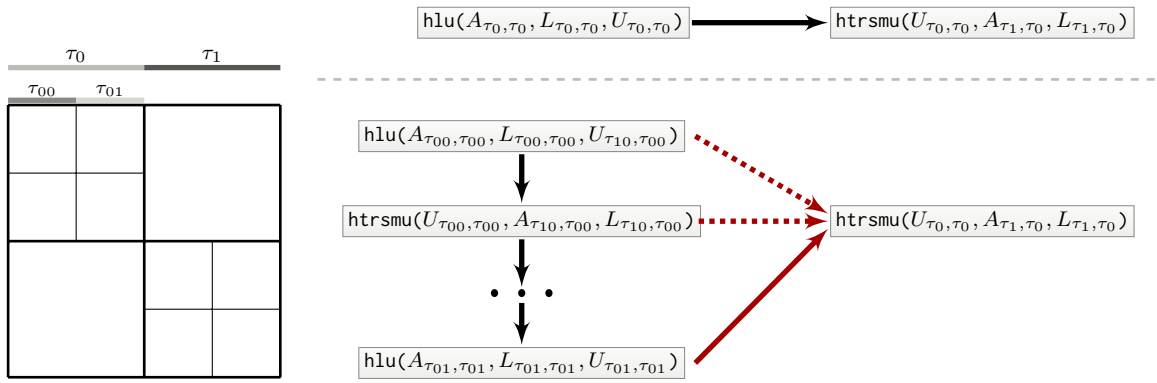


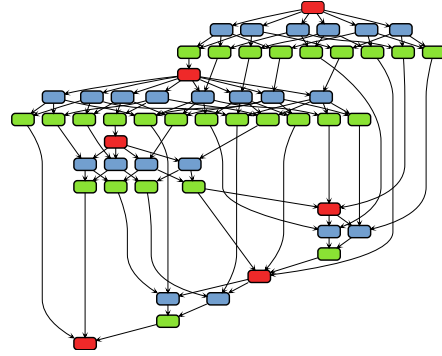
Figure 6: Generation of redundant edges (dotted red) during task refinement.

**Algorithm 12:** Remove redundant edges

```

procedure remove_redundant(in:  $t, N$ , inout:  $S_t$ )
   $A_t := \text{bfs}_2(t, G|_N)$ ;
  for all  $s \in S_t$  do
    if  $s \in A_t$  then  $S_t := S_t \setminus \{s\}$ ;
procedure sparsify(in:  $t$ )
  if  $V_t \neq \emptyset$  then  $N := V_t$ ;
  else  $N := \{t\}$ ;
  for all  $s \in S_t$  do
    if  $V_s \neq \emptyset$  then  $N := N \cup V_s$ ;
    else  $N := N \cup \{s\}$ ;
  if  $V_t \neq \emptyset$  then
    for all  $t' \in S_t$  do
      remove_redundant( $t', N, S_{t'}$ );
  else
    remove_redundant( $t, N, S_t$ );

```

Figure 7:  $\mathcal{H}$ -LU-DAG without redundant edges.

sub-graph to look for redundant edges.

**Remark 4.1** The function  $\text{bfs}_2(t, G')$  returns all nodes visited by a breadth-first search starting at  $t$  within the graph  $G'$  with path lengths at least two.

**Remark 4.2** In practise, the search for descendants in Algorithm 12 may further be limited by a maximal path length for efficiency reasons, thereby trading runtime with a slightly larger edge set. As an example, for standard  $\mathcal{H}$ -LU (without accumulators), already a path length of two resulted in a minimal edge set.

In Figure 7 an example of a task graph before and after removal of redundant edges is shown. There, the number of edges is reduced from 74 to 54.

However, the removal of edges is a heuristical procedure since it may remove important edges, needed to guarantee data dependencies in refined tasks.

The task graph for the accumulator based arithmetic is such a negative example. There, the function  $\text{hlu}$  generates sub-tasks for the shifting of updates applied to the

current matrix block and factorization, matrix solves and updates for its sub-blocks (see Figure 8). Since the tasks for `shift_upd` have data dependencies only in terms of the accumulator matrices, a corresponding `shift_upd` predecessor node is needed to guarantee that refined nodes will maintain the data dependencies needed for applying the accumulator updates.

## 4.2 Parallel DAG Computation

Algorithm 11 has two major loops, first the refinement of the tasks and afterwards the refinement of the dependencies. Both loops permit parallel execution as all performed operations are fully independent only affecting local data. The result is shown in Algorithm 13 (see also Algorithm 11 for the omitted parts).

The situation changes if edge sparsification is applied. For a node  $t$  all non-local nodes, i.e., nodes not in  $V_t$ , in the neighbourhood used to find paths must remain unchanged during the optimization of the edge set. Otherwise, the computation of the paths during the reachability test may result in undefined behaviour. To prevent this, mutices associated with all tasks can be used, which are locked

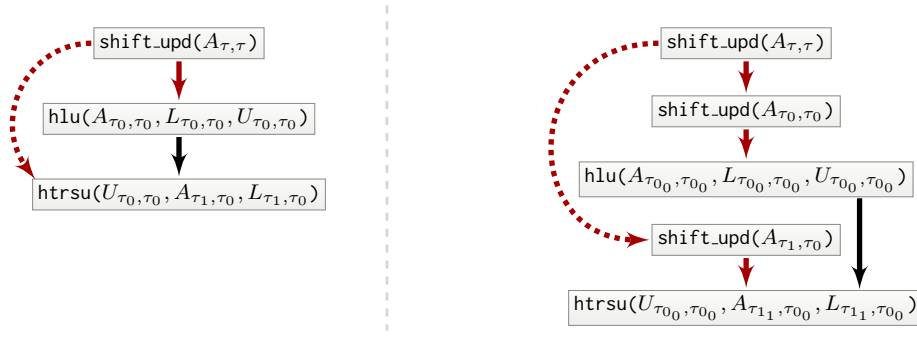


Figure 8: Edges induced by accumulator handling (red) in  $\mathcal{H}$ -LU before (left) and after (right) refinement. The right dotted edge will not be created if left dotted edge would have been removed by sparsification.

#### Algorithm 13: Parallel computation of task graph

```

procedure par_compute_dag(in:  $t$ , out:  $G = (V, E)$ )
   $N := \{t\}$ ;  $V := \emptyset$ ;  $E := \emptyset$ ;
  while  $N \neq \emptyset$  do
    parallel for all  $g \in N$  do
      generate  $V_g, E_g$ ;
     $N' := \emptyset$ ;
    parallel for all  $g \in N$  do
      if  $V_g = \emptyset$  then
        refine local dependencies;
      else
        refine dependencies of sub-tasks;
     $N := N'$ ;

```

before and unlocked after Algorithm 12 for all affected tasks as is shown in Algorithm 14.

#### Algorithm 14: Remove redundant edges with mutices

```

procedure sparsify(in:  $t$ )
  compute neighbourhood  $N$ ;
  for all  $v \in N$  do lock( $v$ );
  if  $V_t \neq \emptyset$  then
    for all  $t' \in S_t$  do
      remove_redundant( $t', N, S_{t'}$ );
  else
    remove_redundant( $t, N, S_t$ );
  for all  $v \in N$  do unlock( $v$ );

```

**Remark 4.3** In Algorithm 13, the details of the loop parallelization were left to the runtime system. In practise, it was more efficient to manually perform the splitting of the task set into separate chunks and perform the parallelization over the resulting set of chunks. If during task refinement such a chunk exceeds a predefined size, it is split into sub-chunks for the next iteration. Similarly, if chunks become too small due to the removal of finished nodes, they are joined with other (small) chunk sets.

**Remark 4.4** The task graph generation from [20] is not so

easily parallelizable as it has to follow the  $\mathcal{H}$ -matrix hierarchy to map the dependencies during  $\mathcal{H}$ -LU correctly. Furthermore, per matrix block only a very few tasks are generated, leaving also little room for parallelization.

### 4.3 Manually merging DAGs for accumulator arithmetic

In Section 3.2 the task graph was generated by following the  $\mathcal{H}$ -LU factorization and creating arithmetic and accumulator tasks for the sub-blocks. The problem with this approach is that two different task graphs, one for the accumulator handling and one for the standard  $\mathcal{H}$ -LU factorization, are created simultaneously. Because of this, more nodes and edges have to be handled at the same time. Furthermore, edge sparsification is not possible (see Section 4.1 and Figure 8).

An alternative approach is to first create only the task graph for `shift_upd` and `apply_upd`. Afterwards the created accumulator tasks are used during the task graph construction for the  $\mathcal{H}$ -LU factorization to explicitly create the dependencies between both graphs, e.g., add a dependency from a `apply_upd` task to a factorization task:

```

procedure hlu(in:  $A_{\tau, \tau}, L_{\tau, \tau}, U_{\tau, \tau}$ )
  if  $(\tau, \tau) \notin \mathcal{L}(T)$  then
    ...
  else
    apply_task( $A_{\tau, \tau}$ )  $\rightarrow$  task( $A_{\tau, \tau} = L_{\tau, \tau} U_{\tau, \tau}$ );

```

Here, `apply_task( $A_{\tau, \sigma}$ )` returns the pre-generated task for `apply_upd` or `shift_upd` corresponding to the matrix block  $A_{\tau, \sigma}$ .

In an analog way, dependencies from `add_upd` (which replaces the `hmul` call) to the corresponding `apply_upd/shift_upd` task are created:

```

procedure hmul(in:  $\alpha, A_{\tau, \rho}, B_{\rho, \sigma}, C_{\tau, \sigma}$ )
  if  $\{(\tau, \rho), (\rho, \sigma), (\tau, \sigma)\} \cap \mathcal{L}(T) = \emptyset$  then
    ...
  else
    task(add_upd( $\alpha, A_{\tau, \rho}, B_{\rho, \sigma}, C_{\tau, \sigma}$ ))  $\rightarrow$ 
    apply_task( $C_{\tau, \sigma}$ );

```

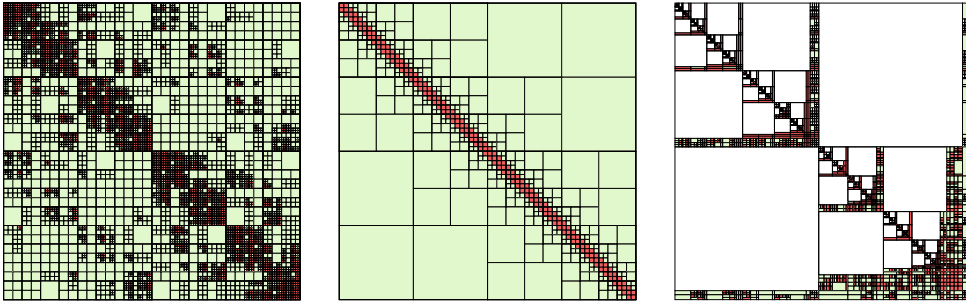


Figure 9: Block structure for model problems: Laplace SLP (left), 1D integral equation (middle) and sparse matrix (right).

Software	Version
HLR	719c48f812e4
HLIBpro	2.7.2
GCC	8.2
Intel TBB	2019.0
Intel MKL	2018.4
jemalloc	5.2.1

Table 3: Versions of software used for the experiments

While this approach does not purely rely on the principle of data dependencies, it is faster since less edges are processed during task graph generation.

## 5 Numerical Experiments

The new semi-automatic task-graph generation will be tested for several different  $\mathcal{H}$ -matrices, which differ by their structure and dimension. For comparison, these test will also be performed for the DAG algorithm from [20], in the following referred to as the *level-wise* method.

Please note, that only the generation of the task-graphs will be tested as the actual DAG execution does not differ between the level-wise and the semi-automatic method. The reason for this is, that the tasks of the DAG are identical and therefore also the computational work. In theory, a difference may exist due to overhead of the runtime system scheduling the different task graphs. However, such a difference was not observed during the experiments.

The versions of the different software used in the tests is shown in Table 3. All tests were performed on a system with two Intel Xeon Gold 6148 CPUs and 192GB of main memory running SLES12 SP4.

**Remark 5.1** *All tests were executed ten times for the same problem. Results in tables will show the median of these results. The diagrams will also use the median for the corresponding plot and will furthermore show the worst/best result as a colored area.*

### 5.1 Model Problems

The standard problem for the numerical examples is based on a boundary element discretization for the Laplace single layer potential (Laplace SLP) while the domain is defined by the unit sphere:

$$\int_{\Gamma} \frac{1}{\|x-y\|} u(y) dy = f(x), \quad x \in \Gamma \quad (1)$$

with  $\Gamma = \{x \in \mathbb{R}^3 : \|x\|_2 = 1\}$ . Piecewise constant ansatz functions are used for the discretization. Furthermore, standard admissibility

$$\min \{\text{diam}(t), \text{diam}(s)\} \leq \eta \text{dist}(\tau, \sigma)$$

is applied for setting up the block tree.

**Remark 5.2** *For all numerical examples, the matrix entries are not of importance as for the computation of the task graph, only the block tree is needed.*

The Laplace SLP model problem will be the default model problem for the numerical experiments below. If not stated otherwise, the data from all figures and tables correspond to this problem.

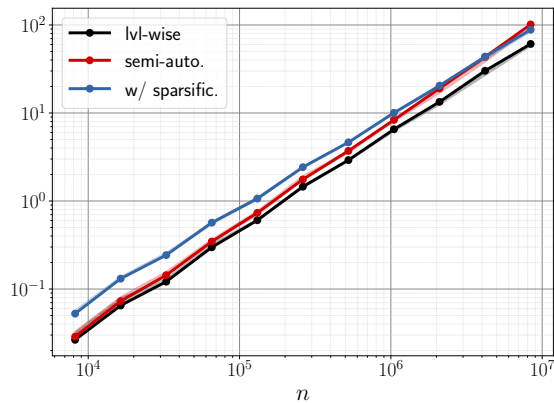
While the block structure of the Laplace SLP problem resembles a typical  $\mathcal{H}$ -matrix block structure and therefore serves as a reasonable approximate for other geometries, we will also consider the standard 1D model problem from [4]:

$$\int_0^1 \log \|x-y\| u(y) dy = f(x), \quad x \in [0, 1] \quad (2)$$

Again, standard admissibility is used for the block tree, which results in a very coarse block structure of the  $\mathcal{H}$ -matrix, corresponding to a very limited number of tasks per level. Therefore, the overhead due to refinement is higher compared to the Laplace SLP example.

The two previous problems use boundary element methods to discretize an integral equation. The last model problem will instead use the finite element method for the partial differential equation

$$-\kappa \Delta u + b \cdot \nabla u = f \quad \text{in } \Omega = ]0, 1[^3. \quad (3)$$



n	level-wise	semi-auto.	w/ sparsific.
8.192	$2.47 \cdot 10^{-2}$ s	$2.91 \cdot 10^{-2}$ s	$5.43 \cdot 10^{-2}$ s
16.384	$6.71 \cdot 10^{-2}$ s	$7.34 \cdot 10^{-2}$ s	$1.35 \cdot 10^{-1}$ s
32.768	$1.22 \cdot 10^{-1}$ s	$1.45 \cdot 10^{-1}$ s	$2.49 \cdot 10^{-1}$ s
65.536	$3.00 \cdot 10^{-1}$ s	$3.53 \cdot 10^{-1}$ s	$5.91 \cdot 10^{-1}$ s
131.072	$6.12 \cdot 10^{-1}$ s	$7.19 \cdot 10^{-1}$ s	$1.10 \cdot 10^0$ s
262.144	$1.48 \cdot 10^0$ s	$1.79 \cdot 10^0$ s	$2.50 \cdot 10^0$ s
524.288	$2.94 \cdot 10^0$ s	$3.68 \cdot 10^0$ s	$4.80 \cdot 10^0$ s
1.048.576	$6.59 \cdot 10^0$ s	$8.43 \cdot 10^0$ s	$1.03 \cdot 10^1$ s
2.097.152	$1.30 \cdot 10^1$ s	$1.90 \cdot 10^1$ s	$2.09 \cdot 10^1$ s
4.194.304	$3.02 \cdot 10^1$ s	$4.36 \cdot 10^1$ s	$4.46 \cdot 10^1$ s
8.388.608	$6.15 \cdot 10^1$ s	$1.02 \cdot 10^2$ s	$9.03 \cdot 10^1$ s

Figure 10: Sequential runtime of level-wise and semi-automatic task graph generation with and without edge sparsification.

n	#nodes	#edges		
		level-wise	semi-auto.	w/ sparsific.
8.192	38.653	212.698	219.494	131.288
16.384	87.346	580.992	611.866	303.133
32.768	150.139	1.169.104	1.284.578	520.694
65.536	321.362	2.819.304	3.214.902	1.115.069
131.072	597.784	5.721.682	6.798.604	2.074.099
262.144	1.346.326	13.848.468	16.926.586	4.687.193
524.288	2.556.413	28.798.228	36.502.620	8.904.326
1.048.576	5.370.314	64.666.356	84.095.200	18.844.125
2.097.152	10.351.022	134.903.680	180.723.520	36.323.779
4.194.304	21.699.437	298.927.488	409.007.162	76.419.056
8.388.608	41.824.170	621.029.914	872.616.702	147.203.171

Table 4: Number of nodes and edges of the DAGs due to level-wise and semi-automatic task graph generation.

with a circular convection direction  $b(v_1, v_2, v_3) := (\frac{1}{2} - v_2, v_1 - \frac{1}{2}, 0)^T$  and  $\kappa = 10^{-2}$ . For the  $\mathcal{H}$ -matrix representation, algebraic nested dissection clustering (see [14]) is used. The resulting block structure is different from the block structure of the Laplace SLP and the 1D problem with a combination of large diagonal blocks, zero off-diagonal blocks and rectangular blocks (see Figure 9).

## 5.2 Comparing semi-automatic and level-wise DAG generation

In Figure 10 the sequential runtime of the level-wise and the semi-automatic algorithms are shown together with the corresponding values for the sphere example.

As expected, the level-wise algorithm shows a faster runtime. The main reason for this is that the semi-automatic approach is more compute intensive due to the many comparisons of data dependencies. Furthermore, the semi-automatic algorithm has a significant management overhead due to memory allocation/deallocation of nodes and edges during task refinement.

**Remark 5.3** *This memory management overhead is also the reason why the memory allocation library jemalloc [18] was used as it resulted in a significant runtime improvement.*

Another reason for the slightly higher runtime is a larger number of edges as can be seen in Table 4. Though the number of nodes differs slightly since the level-wise approach uses additional synchronization nodes for the diagonal factorization tasks, this difference is negligible (about 1–2%).

The number of edges can be decreased significantly by using edge sparsification from Section 4.1. The improvement of the results shown in Table 4 reach a factor of almost 6 at the largest problem size. The number of edges with sparsification is also much smaller than with level-wise DAG construction.

Since edge sparsification involves additional computations, the runtime is normally increased. However, since also the edge set is reduced, the computational savings due to this reduction finally lead to a faster runtime as can be seen in Figure 10.

### 5.3 Parallel DAG generation

The critical issue for the task graph generation is the low computational density of the computation coupled with mainly indirect memory addressing using pointers as the graph data structure needs to be as flexible as possible. Furthermore, the  $\mathcal{H}$ -matrices involved in the arithmetic need to be accessed simultaneously while generating the DAG, thereby competing for memory bandwidth. Therefore, the parallel scaling behaviour is not expected to be ideal.

The results shown in Figure 11 confirm these expectations. The parallel speedup compared to the sequential runtime is limited, achieving only a factor of 4 for a single CPU with 20 cores. When using two CPUs this drops to a speedup of 3 due to more overhead, e.g., slower memory access for non-local data.

Nevertheless, the algorithm benefits from a parallel CPU and achieves maximal speedup already with a few number of CPU cores as is shown in Figure 12, making the semi-automatic DAG generation faster on most computer systems compared to the level-wise DAG generation.

When enabling edge sparsification, the same effect as in the sequential case can be observed, namely that for small problem sizes the additional overhead leads to an increase in the runtime while the reduced number of edges finally result in a faster algorithm. When comparing DAG generation with edge sparsification for sequential and parallel execution, the parallel speedup is also higher as can be seen in Figure 12. This higher speedup is achieved although additional mutices had to be used as explained in Section 4.2. Apparently the increase in computational complexity per task due to the path search leads to a better usage of parallel resources.

However, in both cases, a significant (sequential) overhead limits the achievable speedup, which is further limited by using a second CPU due to a higher communication overhead. However, comparing the parallel runtime even with a few CPU cores with the level-wise approach clearly shows an advantage of the semi-automatic method on practically all computer systems nowadays. This is also shown in Figure 14. There, the runtime percentage of the task graph generation on the full  $\mathcal{H}$ -LU factorization is shown for the Laplace SLP model problem on two CPUs (40 cores) using the best runtime setup for creating the DAG. Since DAG execution scales much better compared to DAG construction, the percentage is rather large. However, the runtime complexity of  $\mathcal{H}$ -LU is higher, leading to a smaller percentage with larger problem sizes, even for the level-wise method. Furthermore, the semi-automatic approach is not only faster compared to the old algorithm, but the relative portion does also shrink faster. Enabling edge sparsification further reduces this part, albeit only for large problem sizes.

**Remark 5.4** *For the DAG execution phase of the  $\mathcal{H}$ -LU factorization, the Laplace SLP example only needs a relatively small amount of floating point operations per index. For*

*other problems, e.g. Helmholtz of Maxwell, the computational costs are much higher, further reducing the percentage of task graph generation on the full  $\mathcal{H}$ -LU factorization.*

For the 1D model problem (2) the general behaviour of the runtime and the number of edges is similar to the Laplace SLP problem. However, due to the limited number of blocks per level and the deeper hierarchy of the  $\mathcal{H}$ -matrix, the overhead of the semi-automatic task refinement is more pronounced. Therefore, the break-even point is achieved for larger problem sizes and the advantage of the semi-automatic method (with or without edge sparsification) is smaller compared to the level-wise methods.

The behaviour changes a little with the sparse matrix example (3) as the percentage of the overhead of the semi-automatic method is similar to the Laplace SLP problem. Furthermore, edge sparsification does not result in a similar improvement as due to the sparse block structure, fewer edges per task are created in the first place<sup>2</sup>.

### 5.4 Accumulator based $\mathcal{H}$ -arithmetic

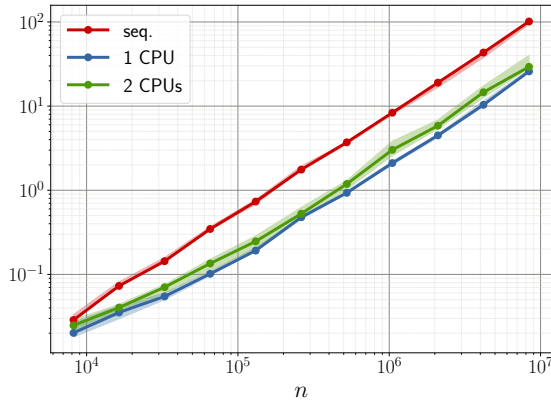
Constructing the task-graph for accumulator based arithmetic leads to similar results for the numerical tests. As is shown in Figure 15, for sequential computations, the level-wise approach is again faster compared to the semi-automatic method. Furthermore, the optimization from Section 4.3 is much faster than the combined approach, where a single DAG is constructed. Therefore, in the following, we will use the merged DAG by default in all experiments.

Compared to the task graph without accumulators, the runtime is slightly faster on all cases, except for edge sparsification. When comparing the number of nodes and edges in the corresponding DAGs, shown in Table 5, it can be seen that the number of nodes has increased due to `apply_upd` and `shift_upd` tasks. However, the number of edges has decreased significantly. The reason is that accumulator handling tasks now bundle update dependencies, which resulted in lots of unnecessary edges without edge sparsification. For the same reason, benefit of edge sparsification is now smaller and with this the overhead of this technique dominates, leading to a much higher runtime.

When using multiple cores the parallel speedup without sparsification is reduced compared to standard  $\mathcal{H}$ -arithmetic. The reason for this behaviour may be due to the reduced number of edges, which further reduces the computational load per node in the graph. The opposite effect slightly increases the parallel speedup in the case that edge sparsification is activated. Since now the number of edges is increased, the amount of work per node is also slightly larger. In both cases, already for small problem sizes, the

<sup>2</sup>For the largest problem size, the level-wise method resulted in 99.969.452 edges, the semi-automatic method used 131.637.777 edges, which was reduced to 30.000.577 edges with edge sparsification, The number of nodes was 11.329.775.





n	Parallel Speedup	
	1 CPU	2 CPUs
8.192	1.42	1.46
16.384	2.16	1.66
32.768	2.96	2.59
65.536	3.30	2.75
131.072	3.69	2.76
262.144	3.93	2.78
524.288	3.95	3.13
1.048.576	3.89	3.12
2.097.152	4.21	2.99
4.194.304	4.16	3.14
8.388.608	3.87	3.43

Figure 11: Parallel runtime using one CPU (20 cores) and two CPUs (40 cores).

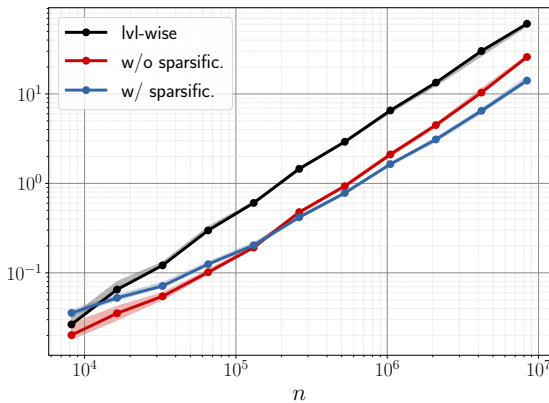


Figure 12: Parallel runtime (left) using one CPU (20 cores) and parallel speedup (right) for  $n = 4.194.304$  with and without edge sparsification.

semi-automatic DAG generation is faster compared to the level-wise approach.

When looking at the relative portion of the DAG construction on the full accumulator based  $\mathcal{H}$ -LU factorization, as shown in Figure 17 for the Laplace SLP problem, again then semi-automatic approach is faster compared to the level-wise method and the percentage is decreasing with larger problems. However, the task graph generation with accumulators takes a significantly larger part in the full  $\mathcal{H}$ -LU factorization compared to standard  $\mathcal{H}$ -arithmetic.

For the 1D model problem (2) the task refinement overhead is even more dominant compared to standard  $\mathcal{H}$ -arithmetic. This results in a higher runtime of semi-automatic task graph generation compared to the level-wise method for all tested problem sizes as is shown in Figure 18 (left).

In case of the sparse matrix example (3), the semi-automatic method is faster than the level-wise approach for middle-sized problems due to less refinement overhead (Figure 18, right).

As for the Laplace SLP problem, also for the 1D model

problem and the sparse matrix, edge sparsification does not result in a lower runtime. Only memory consumption can be reduced.

## 6 Conclusion

We have presented a new task graph generation procedure for  $\mathcal{H}$ -matrix arithmetic, which relies on the standard recursive algorithms and the data dependencies expressed by the block index sets of the involved sub-blocks of the  $\mathcal{H}$ -matrix. This significantly simplifies the implementation of task-based arithmetic for  $\mathcal{H}$ -matrices compared to previous attempts while simultaneously keeping its high performance on many-core systems.

Accumulator based  $\mathcal{H}$ -matrix arithmetic fits naturally into the algorithm and shows excellent results on its own compared to standard arithmetic.

Furthermore, since the new approach also permits parallelization, the task graph generation is also faster on multi- and many-core CPUs compared to the previous, level-wise

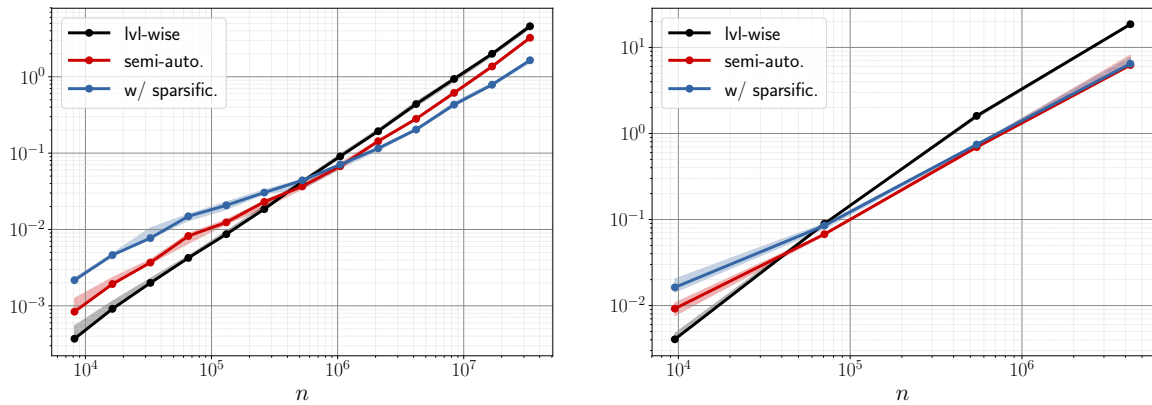


Figure 13: Runtime for one CPU (20 cores) for 1D model problem (2) (left) and PDE problem (3) (right).

n	#nodes	#edges		
		level-wise	semi-auto.	w/ sparsific.
8.192	45.027	174.941	183.218	183.840
16.384	101.584	441.522	474.277	479.169
32.768	177.121	829.991	947.430	963.174
65.536	378.372	1.858.564	2.256.501	2.282.233
131.072	708.698	3.561.068	4.640.641	4.563.089
262.144	1.583.958	8.157.734	11.238.839	10.738.999
524.288	3.019.337	15.919.483	23.627.396	21.654.670
1.048.576	6.325.151	33.913.026	53.345.529	46.811.203
2.097.152	12.220.179	66.666.176	112.490.323	94.020.901
4.194.304	25.543.336	140.856.257	250.940.470	200.095.310
8.388.608	49.346.180	275.508.834	527.100.659	398.294.409

Table 5: Number of nodes and edges of the DAGs due to level-wise and semi-automatic task graph generation for accumulator based  $\mathcal{H}$ -arithmetic.

algorithm. However, the general parallel speedup is limited and needs further investigation into how it can be improved. Though the DAG execution still takes much longer compared to task graph generation, it also scales better with more CPU cores (see [20]). Therefore, for newer CPU generations with even more CPU cores, a better parallel scaling behaviour of the task graph generation is needed to maintain the current portion on the overall – LU factorization procedure.

The next step is the application of the semi-automatic method on variations of the  $\mathcal{H}$ -matrix arithmetic, which were previously not possible or extremely complicated. In fact, one such technique, currently in development and the topic of an upcoming paper was the original motivation to investigate automatic task graph generation.

Another advantage of the semi-automatic approach, not discussed in this work, is the ability for DAG fusion, e.g., the combination of separate task graphs for composed  $\mathcal{H}$ -arithmetic operations like  $\mathcal{H}$ -matrix inversion. This should further increase the parallel efficiency of such operations on multi- and many-core systems.

## References

- [1] J. I. Aliaga, R. Carratalá-Sáez, R. Kriemann, and E. S. Quintana-Orti. “Task-parallel LU factorization of hierarchical matrices using OmpSs”. In: *2017 IEEE 31st international parallel and distributed processing symposium workshops (IPDPSW 2017): proceedings; May 29 2017–June 2 2017; Orlando, Florida, USA*. New York: IEEE, 2017, pp. 1148–1157. ISBN: 978-1-5386-3408-0.
- [2] C. Augonnet, S. Thibault, R. Namyst, and P.-A.; Wacrenier. “StarPU: A Unified Platform for Task Scheduling on Heterogeneous Multicore Architectures”. In: *Concurr. Comput.: Pract. Exper.* 23.2 (Feb. 2011), pp. 187–198. ISSN: 1532-0626.
- [3] S. Börm. “Hierarchical matrix arithmetic with accumulated updates”. In: *arXiv e-prints* (Mar. 2017). arXiv: 1703.09085 [math.NA].
- [4] S. Börm, L. Grasedyck, and W. Hackbusch. *Hierarchical Matrices*. Tech. rep. Lecture note 21, MPI Leipzig, 2003.
- [5] Programming Models Group BSC. *OmpSs*. 2019. URL: <https://pm.bsc.es/omps>.
- [6] Programming Models Group BSC. *OmpSs-2*. 2019. URL: <https://pm.bsc.es/omps-2>.

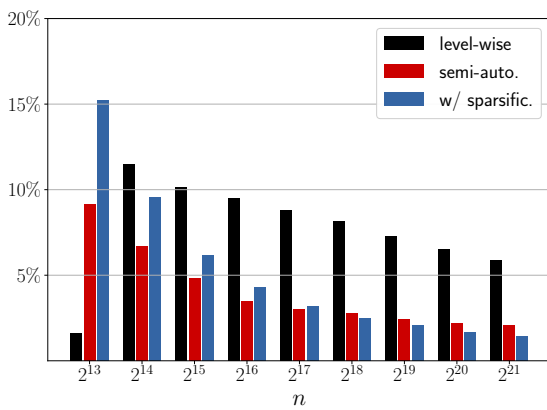
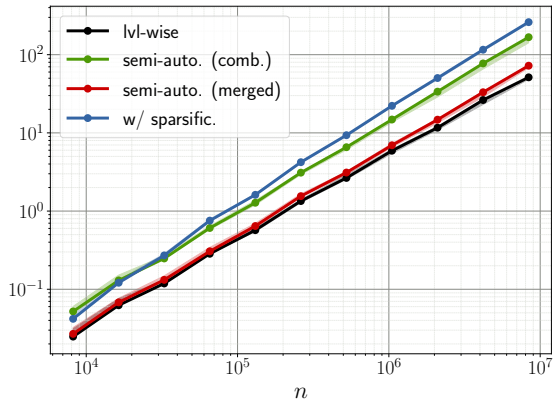


Figure 14: Percentage of task graph generation on full  $\mathcal{H}$ -LU algorithm

- [7] A. Buttari. “Fine-Grained Multithreading for the Multifrontal QR Factorization of Sparse Matrices”. In: *SIAM Journal on Scientific Computing* vol. 35.n° 4 (2013), pp. 323–345.
- [8] A. Buttari, J. Langou, J. Kurzak, and J. Dongarra. “Parallel tiled QR factorization for multicore architectures”. In: *Concurrency and Computation: Practice and Experience* 20.13 (2008), pp. 1573–1590.
- [9] A. Buttari, J. Langou, J. Kurzak, and J. Dongarra. “A class of parallel tiled linear algebra algorithms for multicore architectures”. In: *Parallel Computing* 35.1 (2009), pp. 38–53.
- [10] R. Carratalá-Sáez et al. “Exploiting nested task-parallelism in the  $\mathcal{H}$ -LU factorization”. In: *Journal of Computational Science* 33 (2019), pp. 20–33. issn: 1877-7503.
- [11] L. Dagum and R. Menon. “OpenMP: an industry standard API for shared-memory programming”. In: *Computational Science & Engineering, IEEE* 5.1 (1998), pp. 46–55.
- [12] J. Dölz, H. Harbrecht, and M.D. Multerer. “On the Best Approximation of the Hierarchical Matrix Product”. In: *SIAM J. Matrix Analysis Applications* 40.1 (2019), pp. 147–174.
- [13] L. Grasedyck and W. Hackbusch. “Construction and arithmetics of  $\mathcal{H}$ -matrices”. In: *Computing* 70 (2003), pp. 295–334.
- [14] L. Grasedyck, R. Kriemann, and S. LeBorne. “Parallel black box  $\mathcal{H}$ -LU preconditioning for elliptic boundary value problems”. In: *Computing and visualization in science* 11.4-6 (2008), pp. 273–291. issn: 1432-9360.
- [15] W. Hackbusch. “A sparse matrix arithmetic based on  $\mathcal{H}$ -Matrices. Part I: Introduction to  $\mathcal{H}$ -Matrices”. In: *Computing* 62 (1999), pp. 89–108.
- [16] W. Hackbusch. *Hierarchical Matrices: Algorithms and Analysis*. Vol. 49. Springer Series in Computational Mathematics. Berlin, Heidelberg: Springer, 2015.
- [17] J. Hogg, J. Reid, and J. Scott. “Design of a Multicore Sparse Cholesky Factorization Using DAGs”. In: *SIAM Journal on Scientific Computing* 32.6 (2010), pp. 3627–3649.
- [18] jemalloc. 2019. URL: <http://jemalloc.net/>.
- [19] R. Kriemann. “Parallel  $\mathcal{H}$ -matrix arithmetics on shared memory systems”. In: *Computing* 74 (2005), pp. 273–297.
- [20] R. Kriemann. “ $\mathcal{H}$ -LU factorization on many-core systems”. In: *Computing and Visualization in Science* 16.3 (June 2013), pp. 105–117. issn: 1433-0369.
- [21] R. Kriemann. *HLR*. Aug. 2019. URL: <https://hlibpro.com/hlr>.
- [22] X. Lacoste et al. *Sparse direct solvers with accelerators over DAG runtimes*. Rapport de recherche RR-7972. INRIA, 2012, p. 11. URL: <http://hal.inria.fr/hal-00700066>.
- [23] OpenMP Architecture Review Board. “OpenMP Application Program Interface Version 4.0”. July 2013. URL: <http://www.openmp.org/mp-documents/OpenMP4.0.0.pdf>.
- [24] J. M. Perez, V. Beltran, J. Labarta, and E. Ayguadé. “Improving the Integration of Task Nesting and Dependencies in OpenMP”. In: *2017 IEEE International Parallel and Distributed Processing Symposium (IPDPS)*. May 2017, pp. 809–818.
- [25] S. Thibault. “On Runtime Systems for Task-based Programming on Heterogeneous Platforms”. Habilitation à diriger des recherches. Université de Bordeaux, Dec. 2018.



$n$	level-wise	semi-auto.	w/ sparsific.
8.192	$2.29 \cdot 10^{-2}$ s	$2.70 \cdot 10^{-2}$ s	$4.19 \cdot 10^{-2}$ s
16.384	$6.28 \cdot 10^{-2}$ s	$6.86 \cdot 10^{-2}$ s	$1.21 \cdot 10^{-1}$ s
32.768	$1.20 \cdot 10^{-1}$ s	$1.35 \cdot 10^{-1}$ s	$2.71 \cdot 10^{-1}$ s
65.536	$2.90 \cdot 10^{-1}$ s	$3.16 \cdot 10^{-1}$ s	$7.55 \cdot 10^{-1}$ s
131.072	$5.64 \cdot 10^{-1}$ s	$6.71 \cdot 10^{-1}$ s	$1.61 \cdot 10^0$ s
262.144	$1.36 \cdot 10^0$ s	$1.57 \cdot 10^0$ s	$4.22 \cdot 10^0$ s
524.288	$2.67 \cdot 10^0$ s	$3.20 \cdot 10^0$ s	$9.34 \cdot 10^0$ s
1.048.576	$5.90 \cdot 10^0$ s	$7.08 \cdot 10^0$ s	$2.22 \cdot 10^1$ s
2.097.152	$1.18 \cdot 10^1$ s	$1.49 \cdot 10^1$ s	$5.03 \cdot 10^1$ s
4.194.304	$2.64 \cdot 10^1$ s	$3.37 \cdot 10^1$ s	$1.16 \cdot 10^2$ s
8.388.608	$5.21 \cdot 10^1$ s	$7.47 \cdot 10^1$ s	$2.61 \cdot 10^2$ s

Figure 15: Sequential runtime of level-wise and semi-automatic task graph generation for accumulator based  $\mathcal{H}$ -arithmetic.

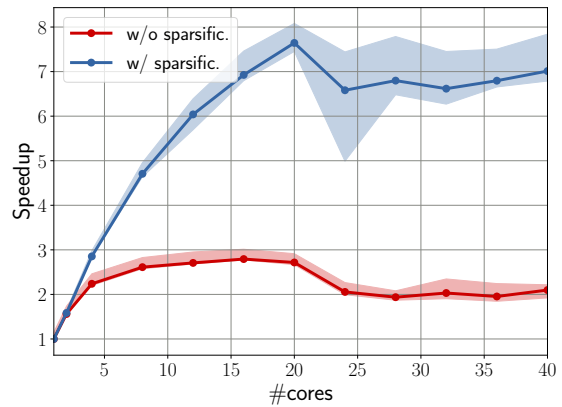
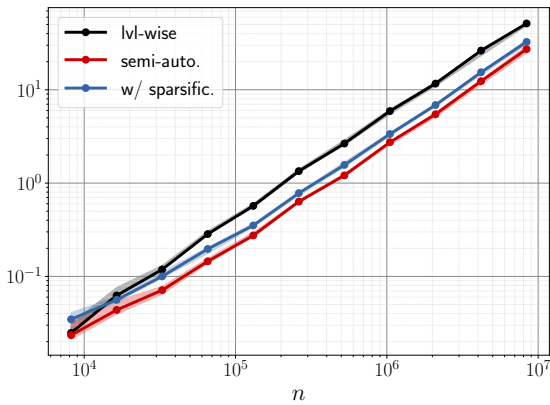


Figure 16: Parallel runtime using one CPU (20 cores, left) and parallel speedup (right) of task graph generation for accumulator based  $\mathcal{H}$ -arithmetic.

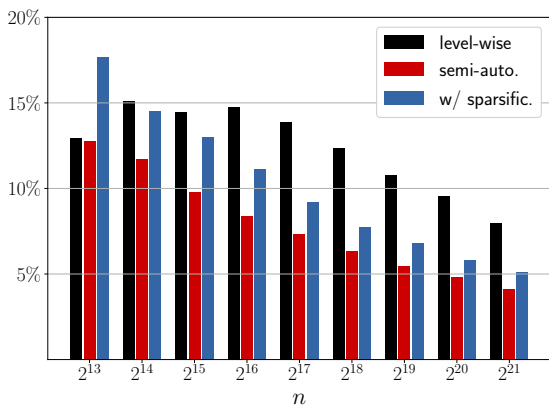


Figure 17: Runtime percentage of task graph generation for entire accumulator based  $\mathcal{H}$ -LU algorithm.

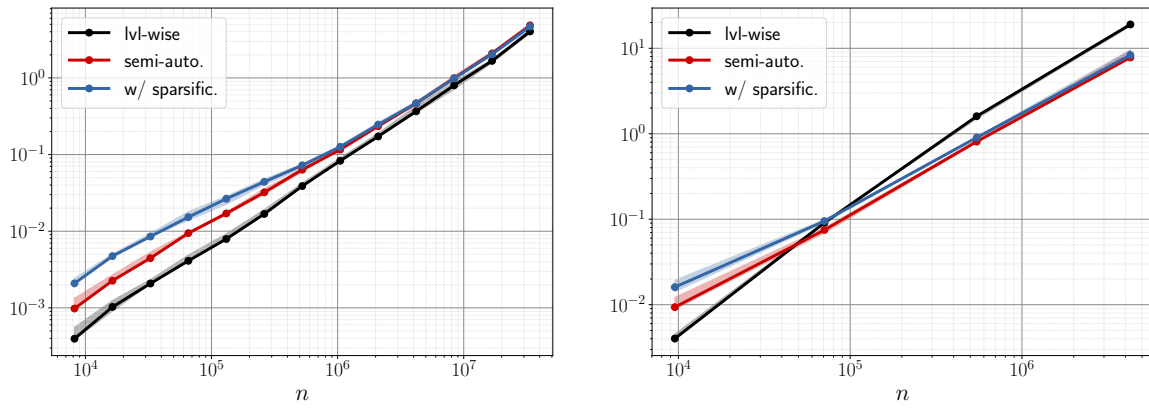


Figure 18: Best runtime for task graph generation with accumulators for the 1D model problem (left) and the sparse matrix (right).